JACC: BASIC TO TRANSLATIONAL SCIENCE
VOL. 1, NO. 6, 2016
ISSN 2452-302X
http://dx.doi.org/10.1016/j.jacbts.2016.08.006

PRECLINICAL RESEARCH

Serial Coronary Imaging of Early Atherosclerosis Development in Fast-Food-Fed Diabetic and Nondiabetic Swine

Nienke S. van Ditzhuijzen, MSc,[a] Mieke van den Heuvel, MD,[a] Oana Sorop, PhD,[a] Alexia Rossi, MD, PhD,[b] Timothy Veldhof, MSc,[a] Nico Bruining, PhD,[a] Stefan Roest, BSc,[a] Jurgen M.R. Ligthart, RT,[a] Karen Th. Witberg, CCRN,[a] Marcel L. Dijkshoorn, BSc,[a] Koen Nieman, MD, PhD,[a] Monique T. Mulder, PhD,[c] Felix Zijlstra, MD, PhD,[a] Dirk J. Duncker, MD, PhD,[a] Heleen M.M. van Beusekom, PhD,[a] Evelyn Regar, MD, PhD[a]

VISUAL ABSTRACT

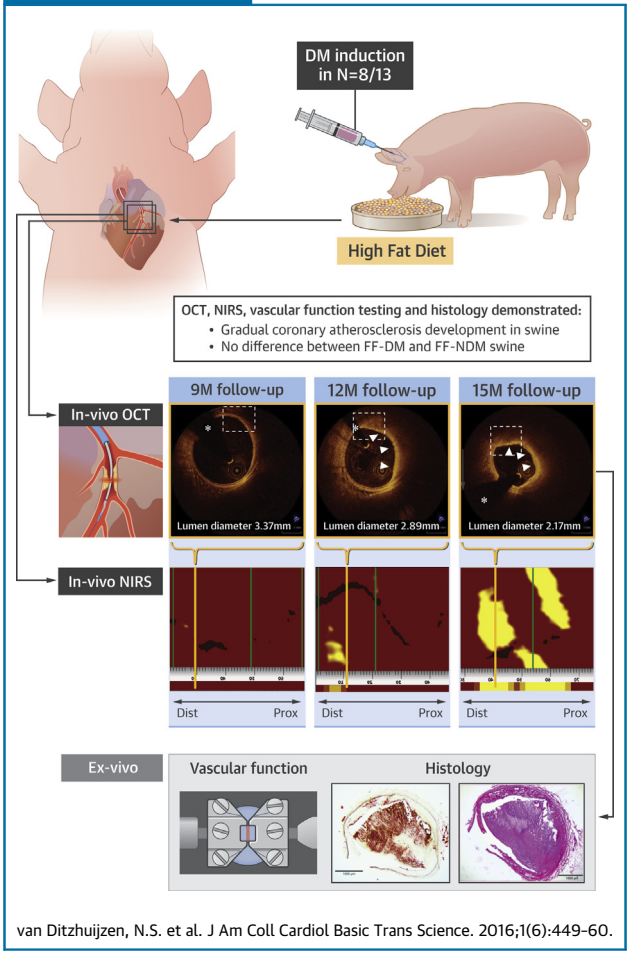

van Ditzhuijzen, N.S. et al. J Am Coll Cardiol Basic Trans Science. 2016;1(6):449-60.

HIGHLIGHTS

In swine with and without diabetes mellitus fed a fast-food diet:

- **OCT, NIRS, CCTA, vascular function testing, and histology can be consecutively and longitudinally performed to assess gradual coronary atherosclerosis development**
- **OCT and NIRS enabled detailed assessment of early coronary atherosclerosis development, whereas CCTA was not able to detect discrete early atherosclerotic changes.**
- **OCT, NIRS, vascular function testing, and histology demonstrated no differences in early atherosclerosis development.**

JACC: BASIC TO TRANSLATIONAL SCIENCE VOL. 1, NO. 6, 2016
OCTOBER 2016:449–60

ABBREVIATIONS AND ACRONYMS

CCTA = coronary computed tomography angiography

DM = diabetes mellitus

FF = fast-food-fed

FIT = fibrous intimal thickening

LCP = lipid core plaque

LL = lipid-laden

NDM = no/non-diabetes mellitus

NIRS = near-infrared spectroscopy

OCT = optical coherence tomography

QCA = quantitative coronary angiography

SNAP = S-nitroso-N-acetylpenicillamine

SUMMARY

Patients with diabetes mellitus (DM) are at increased risk for atherosclerosis-related events compared to non-DM (NDM) patients. With an expected worldwide epidemic of DM, early detection of anatomic and functional coronary atherosclerotic changes is gaining attention. To improve our understanding of early atherosclerosis development, we studied a swine model that gradually developed coronary atherosclerosis. Interestingly, optical coherence tomography, near-infrared spectroscopy (NIRS), vascular function, and histology demonstrated no differences between development of early atherosclerosis in fast-food-fed (FF) DM swine and that in FF-NDM swine. Coronary computed tomography angiography did not detect early atherosclerosis, but optical coherence tomography and near-infrared spectroscopy demonstrated coronary atherosclerosis development in FF-DM and FF-NDM swine. (J Am Coll Cardiol Basic Trans Science 2016;1:449–60)

Patients with diabetes mellitus (DM) have a 2- to 6-fold increased risk of encountering atherosclerosis-related events compared to their non-DM (NDM) counterparts (1). With a worldwide DM epidemic expected, early detection of anatomical and functional atherosclerotic changes in the coronary vasculature is gaining attention. However, patients typically present to the clinician with advanced atherosclerotic disease, thus complicating the study of early atherosclerosis development.

Animal models may provide a solution. Several small animal models, such as a rodent model, have been used to unravel disease mechanisms of coronary artery disease, but their ability to mimic human coronary artery disease is limited (2). The swine coronary artery model can be especially suitable for evaluation of human-like coronary artery disease development. First, the anatomy and physiology of swine hearts are similar to those of human hearts. Second, swine can be rendered diabetic by injection of streptozotocin. Third, patient-like spontaneous coronary atherosclerosis development can be mimicked by additionally feeding the swine a high-cholesterol, high-sugar diet (3); and fourth, in vivo longitudinal invasive and noninvasive imaging can be performed using imaging techniques such as optical coherence tomography (OCT), near-infrared spectroscopy (NIRS), and coronary computed tomography angiography (CCTA) (4). Ex vivo coronary endothelial function can be tested to compare functional with morphological coronary changes, and histology can be performed to assess the magnitude of coronary and aortic atherosclerosis at different time points (4,5).

Because there is little understanding about whether DM affects atherosclerosis development at the onset of coronary artery disease, the aim of our observational study was to assess whether DM affects early atherosclerosis development as assessed by OCT, NIRS, and CCTA in swine fed a high-cholesterol, high sugar ("fast-food") diet.

METHODS

This experimental study was approved by the Erasmus Medical Center Animal Ethics committee and performed in accordance with the Guide for Care and Use of Laboratory Animals (6).

See the Supplemental Appendix for a detailed description of all anaesthesia procedures. Thirteen male crossbred (Yorkshire × Landrace) swine ~11 weeks of age, with an average weight of ~30 kg were included. DM was induced in 8 randomly selected anesthetized swine by streptozotocin (single-dose intravenous injection, 140 mg/kg) (4). All swine were given a fast-food-fed (FF) diet containing 10% sucrose, 15% fructose, 25% (swine) lard, 1% cholesterol, and 0.7% sodium cholate (bile salts). Follow-up

From the [a]Department of Cardiology, Thoraxcenter, Cardiovascular Research School COEUR, Erasmus University Medical Center, Rotterdam, the Netherlands; [b]Department of Radiology, Erasmus University Medical Center, Rotterdam, the Netherlands; and the [c]Department of Internal Medicine, Erasmus University Medical Center, Rotterdam, the Netherlands. Dr. Dijkshoorn is a consultant for Siemens Healthcare. Dr. Regar has received research support from St. Jude Medical through her institution. All other authors have reported that they have no relationships relevant to the contents of this paper to disclose.

Manuscript received April 4, 2016; revised manuscript received August 5, 2016, accepted August 22, 2016.

FIGURE 1 Study Flow Chart and Matching of Invasive Imaging

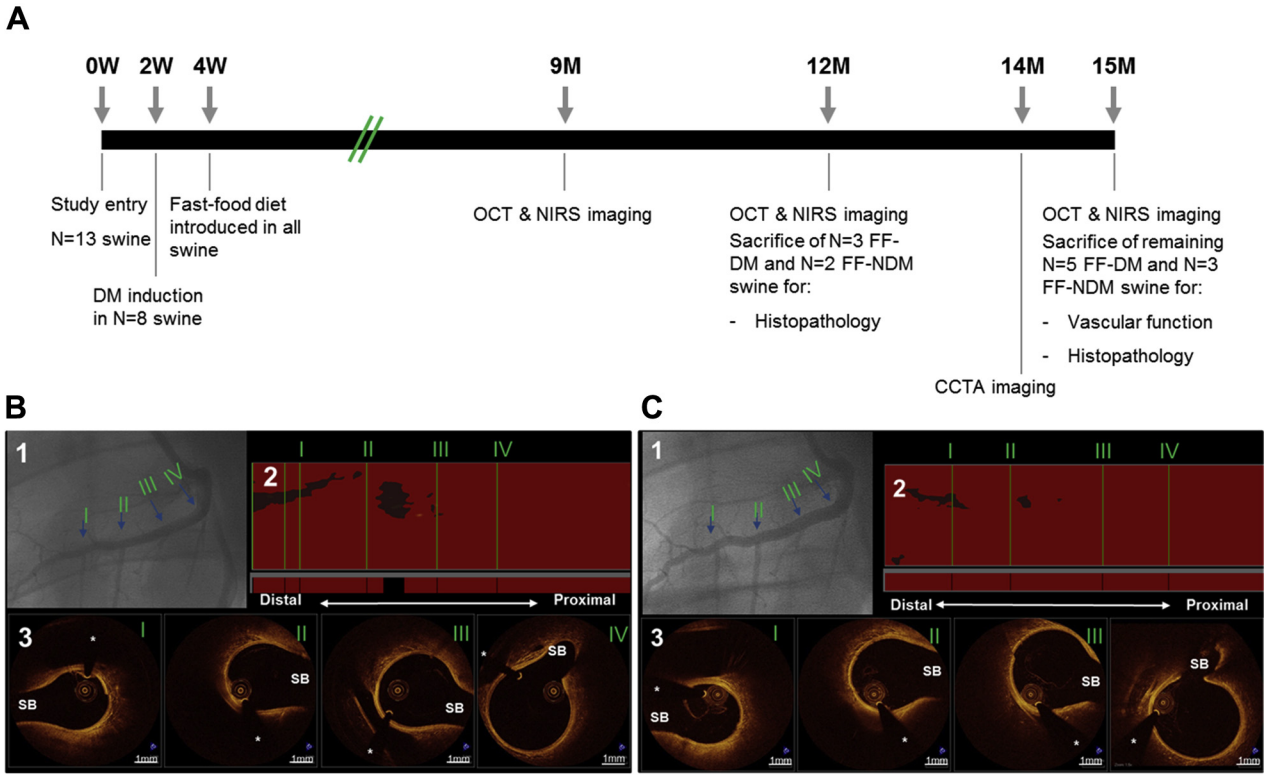

Study flow chart **(A)** and matching of invasive imaging **(B and C)**. The coronary angiograms **(B1 and C1)** were used to match the OCT **(B3 and C3)** and NIRS pullbacks **(B2 and C2)** within and at the various time points. Large side branches on the coronary angiogram **(I to IV)** were indicated on the NIRS chemogram **(B2 and C2, green lines, I to IV)** and matched to the OCT cross-sections **(B3 and C3, I to IV)**. *Guidewire. FF-DM = fast-food-fed swine with diabetes mellitus; FF- NDM = fast-food-fed swine without diabetes mellitus; M = month; NIRS = near-infrared spectroscopy; OCT = optical coherence tomography; SB = side branch; W = weeks.

duration was 12 months (n = 8 FF-DM swine; n = 5 FF-NDM swine) or 15 months (n = 5 FF-DM swine; n = 3 FF-NDM swine), during which similar growth patterns were achieved by adjusting individual caloric intake. See **Figure 1A** for the study flow chart.

Arterial access was obtained by introducing a 9-F sheath into the carotid artery to monitor blood pressure and obtain fasting blood samples to assess plasma insulin, glucose, triglyceride, total cholesterol (TC), low-density lipoprotein (LDL), and high-density lipoprotein (HDL) cholesterol levels and lipoprotein profiles. As control, fasting blood samples were taken from 5 weight-, age-, and sex-matched crossbred swine fed standard chow. In FF-DM swine, blood glucose and ketone levels were monitored weekly by 24-h urine samples, and insulin was administered when needed to prevent ketoacidosis. To obtain lipoprotein profiles, we used density gradient ultracentrifugation and measured cholesterol and triglyceride concentrations spectrophotometrically in the fractions in FF-DM (n = 7), FF-NDM (n = 3), and 1 age-, weight-, and sex-matched control swine (please see Supplemental Appendix for detailed methodology).

To evaluate insulin sensitivity, we calculated the quantitative insulin sensitivity check index, (QUICKI), as $[1/[(\log(I_o) + \log(G_o)]$, in which I_o is the fasting plasma insulin level in μU/ml, and G_o is the fasting blood glucose level in mg/dl, at 9, 12, and 15 months.

IN VIVO OCT, NIRS, AND CCTA. Serial OCT (C7XR FD system; St. Jude Medical, St. Paul, Minnesota) and NIRS (InfraReDx; Nipro, Osaka, Japan) were performed to assess the coronary arteries at 9, 12, and 15 months. The region of interest was defined as the region in which both the OCT and NIRS were available at all 2 time points (9 and 12 months) or all 3 time points (9, 12, and 15 months) and divided

FIGURE 2 Early Atherosclerosis Development in FF-DM and FF-NDM Swine

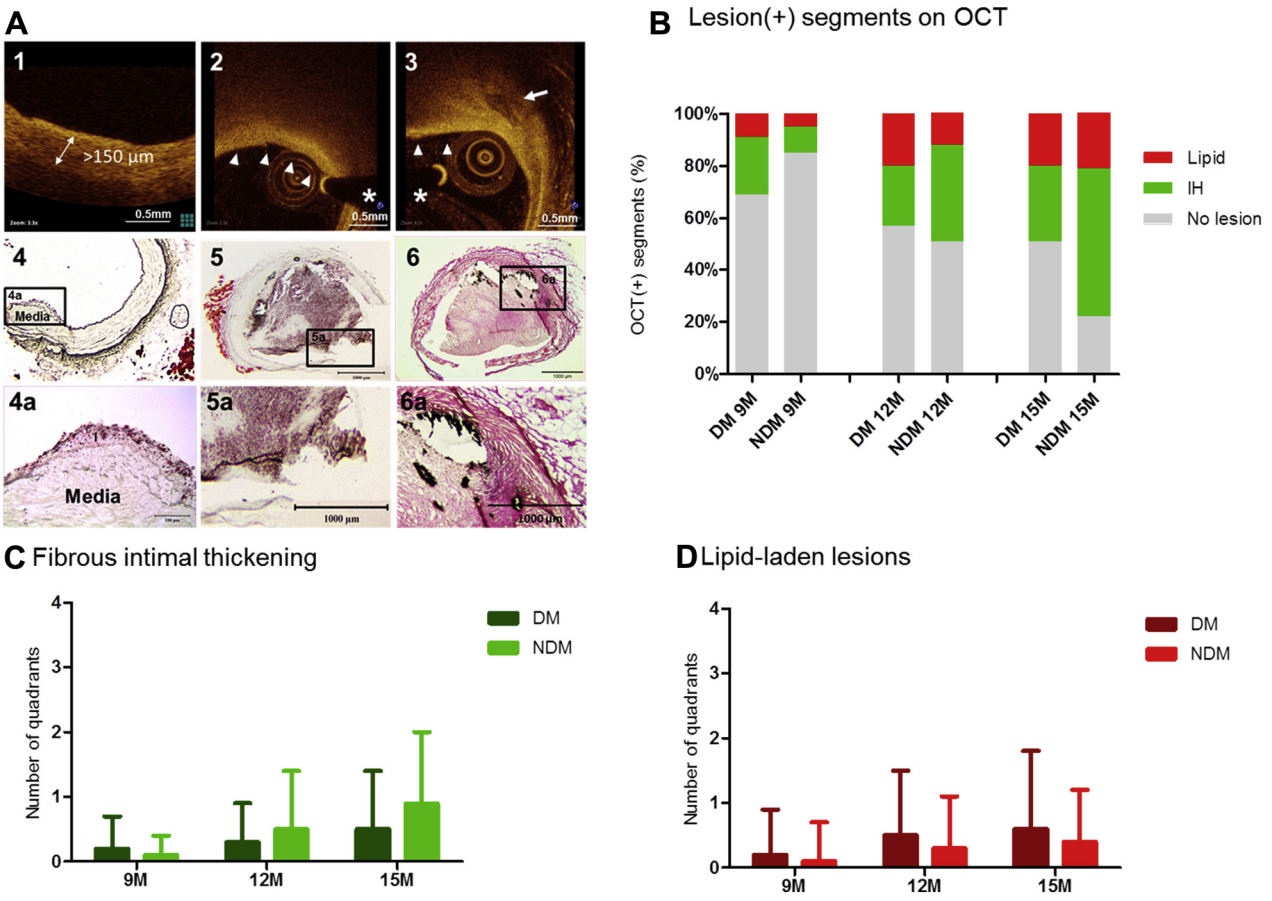

Several lesion types were assessed by OCT **(A1 to A3)** and matched with histology (oil-red-O stain **[A4 and A5]** and von Kossa stain **[A6]**). Intimal hyperplasia was defined as a fibrous lesion >150-µm thickness on OCT **(A1)**, a lipid-laden lesion **(A2 and A5)** as diffusely delineated signal-poor region **(A2, arrowheads)** and a mixed lesion **(A3 and A6)** as a lesion containing both lipid **(A3, arrowheads)** and calcium, which was defined as a sharply delineated signal-poor region **([A3] arrow)**. In histology, red stain denotes lipid **(A5)**, and closed bars denote calcium **(A6)** deposits. **(B)** The prevalence and burden **(C and D)** of disease increased from 9 to 15 months, without any significant differences between FF-DM and FF-NDM. *Guidewire artifact. Abbreviations as in Figure 1.

into 5-mm subsegments. On the NIRS chemogram, side branches were marked during image acquisition based on the location of the catheter in the coronary angiogram. Afterwards, NIRS and angiographically determined side branches were matched to side branches visible in the OCT pullback (**Figures 1B and 1C**).

See Supplemental Appendix for the OCT acquisition methods. Mean lumen area and diameter and minimum lumen diameter were documented for every frame within the region of interest using Curad vessel analysis software (Curad, Maastricht, the Netherlands).

OCT TISSUE CLASSIFICATION. The incidence of lesion-positive subsegments was noted, with lesions classified as fibrous intimal thickening (FIT), lipid-laden (LL), calcified, or mixed (**Figure 2A**), as published previously (7,8) (see Supplemental Appendix for lesion definitions). According to the lesion, lesion burden was calculated as the average number of lesion-positive quadrants (see the Supplemental Appendix for lesion definitions).

For NIRS, the catheter was withdrawn automatically with 0.5 mm/s pullback speed. Within the region of interest, NIRS documented the probability that lipid core plaque (LCP) was present. The data are displayed in a 2-dimensional arterial map, the chemogram. A summary of the results for each 2 mm of artery is computed (block chemogram) and mapped to a color scale with 4 discrete

colors. The colors correspond to the probability that LCP is present, with red indicating low probability and yellow high probability (red = $p \leq 0.57$; orange = 0.57; $\leq p < 0.84$; tan = $0.84 \leq p < 0.98$; yellow = $p \geq 0.98$) (9). In the current analysis, yellow, tan, or orange blocks were considered NIRS-positive.

See the Supplemental Appendix for description of the CCTA acquisition methods. CCTA was performed using the electrocardiography (ECG)-gated spiral scan mode. Data sets with optimal image quality were reconstructed mainly in the mid- to end-diastolic phase, with a slice thickness of 0.75 mm at an increment of 0.4 mm. Coronary lesions were classified as high-density or low-density as described previously (10). High-density was recognized as >220 HU, low density as <220 HU.

EX VIVO ASSESSMENT. Sacrifice was scheduled after imaging at 12 months (n = 3 FF-DM, n = 2 FF-NDM) or 15 months (n = 5 FF-DM, n = 3 FF-NDM). The hearts were removed, and the coronary tree was dissected free and placed in cold, oxygenated Krebs bicarbonate buffer solution or fixed in formalin.

Vascular function. To assess coronary endothelial function at 15 months, segments of coronary arteries (~4 mm in length) were suspended in organ baths. Vascular responses were measured as changes in isometric force to different concentrations of vasoactive substances, as described previously using pEC_{50} values (11–13). Endothelium-dependent relaxation to bradykinin (BK; 10^{-10} to 10^{-6} mol/l) was recorded upon pre-constriction with the thromboxane analog U46619 (10^{-6} mol/l). Similarly, endothelium-independent vasodilation to *S*-nitroso-*N*-acetylpenicillamine (SNAP; 10^{-9} to 10^{-5} mol/l) and endothelium-dependent vasoconstriction to endothelin-1 (10^{-10} to 10^{-7} mol/l) were assessed.

Histology. The remaining coronary artery segments were used for histological analysis. Two-millimeter segments taken from areas that demonstrated vascular wall changes by coronary angiography or OCT were embedded in optimal cutting temperature compound and then frozen. Tissue sections were cut and stained with hematoxylin-eosin as an overview stain, with oil-red-O (Abcam, Cambridge, United Kingdom) for lipid, and with von Kossa for calcium. The sections were matched with OCT and NIRS images by using angiographic images, pullback length, and arterial landmarks. Abdominal aortae were harvested and stained en face by oil-red-O to assess atherosclerotic burden, expressed as a percentage of stained area to total area.

STATISTICAL ANALYSIS. SPSS version 20.0 software (Chicago, Illinois) was used for statistical analysis. Normally distributed data are mean ± SD. For swine-level analysis, an independent sample Student *t* test was used, and for segment-level analysis, generalized estimating equations modeling was used. For swine-level repeated measures, repeated-measures analysis of variance and for segment-level generalized estimating equations modeling were performed using a linear response model with an autoregressive (1) structure for the within-cluster correlation matrix. A p value of <0.05 was considered statistically significant.

RESULTS

In all 13 swine plasma measurements were obtained. In **Figure 3A**, average plasma insulin, glucose, and cholesterol levels at the time of anesthesia were documented at 9, 12, and 15 months. TC, LDL, HDL, and triglyceride levels were higher in FF-DM and FF-NDM swine than in age-, weight-, and sex-matched control swine (TC: 2.14 ± 0.6 mmol/l; HDL: 0.94 ± 0.2 mmol/l; LDL: 1.22 ± 0.6 mmol/l; triglycerides: 0.20 ± 0.1 mmol/l). DM was successfully induced, as indicated by higher glucose levels in FF-DM than in FF-NDM swine ($p < 0.05$), and glucose levels remained fairly stable over time (**Figure 3B**). Mean arterial pressures were similar between FF-DM and FF-NDM swine at 15 months (89 ± 10 mm Hg, 85 ± 5 mm Hg, respectively; $p > 0.10$), and, because similar growth patterns were maintained by monitoring individual caloric intake (**Figure 3C**), mean final weights were comparable (FF-DM: 97.3 ± 7.3 kg; FF-NDM: 96.5 ± 3.3 kg; $p = 0.87$). Moreover, we created hyperglycemic levels in FF-DM swine without evidence of hypoglycemia.

Because lipoprotein profiles were comparable at 9, 12, and 15 months, all lipid profiles for FF-DM and FF-NDM swine were combined. LDL and triglycerides were higher and HDL lower in FF-DM and FF-NDM swine compared with an age-, weight-, and sex-matched control. Furthermore, the LDL peak was dramatically increased and shifted to the right in FF-DM and FF-NDM swine compared with control, indicating a lower density of LDL (Supplemental Figure 1).

QUICKI results were slightly lower in FF-DM swine (0.56 ± 0.10 at 9 months, 0.69 ± 0.14 at 12 months, and 0.53 ± 0.03 at 15 months) than in FF-NDM swine at 9 and 15 months (0.68 ± 0.11 at 9 months; 0.72 ± 0.14 at 12 months; and 0.60 ± 0.04 at 15 months; $p = 0.04$ at 9 months; $p = 0.69$ at 12 months; and $p = 0.02$ at 15 months). Compared with age-, weight-,

FIGURE 3 Plasma Measurement Results and Individual Insulin and Food Administration

A

	9M			12M			15M		
	FF-DM (n=8)	FF-NDM (n=5)	P-value *	FF-DM (n=8)	FF-NDM (n=5)	P-value *	FF-DM (n=5)	FF-NDM (n=3)	P-value*
Plasma measurements									
Glucose, mmol/L	15.31±8.08	4.38±0.66	0.01	12.96±6.43	4.7±1.44	0.01	17.64±10.15	5.37±1.22	0.09
Insulin, µ/mL	0.28±0.07	0.44±0.18	0.04	0.19±0.15	0.36±0.20	0.12	0.35±0.26	0.52±0.07	0.33
Total cholesterol, mmol/L	20.30±5.75	17.84±5.10	0.45	18.23±4.97	15.84±2.38	0.34	16.82±3.83	14.33±4.16	0.42
LDL, mmol/L	16.57±5.41	14.63±4.56	0.52	14.63±0.57	12.67±1.95	0.39	13.63±3.82	11.30±3.54	0.43
HDL, mmol/L	5.22±0.63	5.64±0.55	0.26	5.68±0.87	5.33±0.60	0.46	5.12±0.90	5.27±0.68	0.81
Triglycerides, mmol/L	1.15±0.73	0.43±0.22	0.03	0.95±0.71	0.37±0.20	0.06	1.26±1.12	0.35±0.07	0.14

B

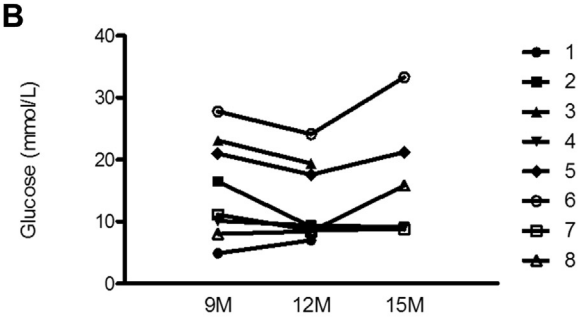

C

Animal	1	2	3	4	5	6	7	8	9	10	11	12	13
Sacrifice moment	12M	12M	12M	15M	15M	15M	15M	15M	12M	12M	15M	15M	15M
Frequency of insulin given	8	8	47	12	9	56	8	8	-	-	-	-	-
Total insulin given (U)	70	70	357	120	85	489	70	70	-	-	-	-	-
Average diet (gram/week)	661± 84	738± 83	873± 79	793± 80	786 ± 97	1295± 316	690± 99	725± 86	634± 63	589± 69	661± 73	661± 92	673± 86

Plasma measurement results **(A and B)** and individual insulin and food administration **(C)**. Data are mean ± SD. Animals 1 to 8 are FF-DM; 9 to 13 are FF-NDM. 9M = 9-month follow-up; 12M = 12-month follow-up; 15M = 15-month follow-up. *p value = comparison between FF-DM and FF-NDM swine.

and sex-matched control swine, QUICKI results were reduced in both the FF-DM and the FF-NDM swine at 9 months ($p = 0.02$) and 15 months ($p < 0.01$), suggesting that insulin resistance occurred due to experimentally induced islet dysfunction as well as the FF diet.

OCT, NIRS, AND CCTA FINDINGS. Serial 9- and 12-month OCT and NIRS were performed in 12 of 13 swine, and additional 15-month evaluations were performed in 7 of 8 swine. Due to technical difficulties, NIRS could not be performed in 1 swine at 9 months, which was excluded from analysis. Additionally, 1 swine died during imaging at 15 months due to a technical complication that caused myocardial ischemia. CCTA was performed in all 8 swine at 14 months ($n = 5$ FF-DM, $n = 3$ FF-NDM).

Mean and minimal lumen diameters decreased slightly from 9 to 15 months in all swine ($p > 0.10$), without a significant difference between FF-DM and FF-NDM swine ($p > 0.10$) (Supplemental Table 1).

OCT demonstrated focal lesions that were highly variable in presence, location, and morphology. Between FF-DM and FF-NDM, there were no differences regarding lesion type ($p = 0.42$ for FIT; $p = 0.77$ for LL) or burden ($p = 0.17$ for intimal hyperplasia; $p = 0.49$ for LL), except for 1 mixed lesion that developed in an FF-DM swine with a

FIGURE 4 Lipid-Containing Lesion Development Observed by OCT, NIRS, and Histology

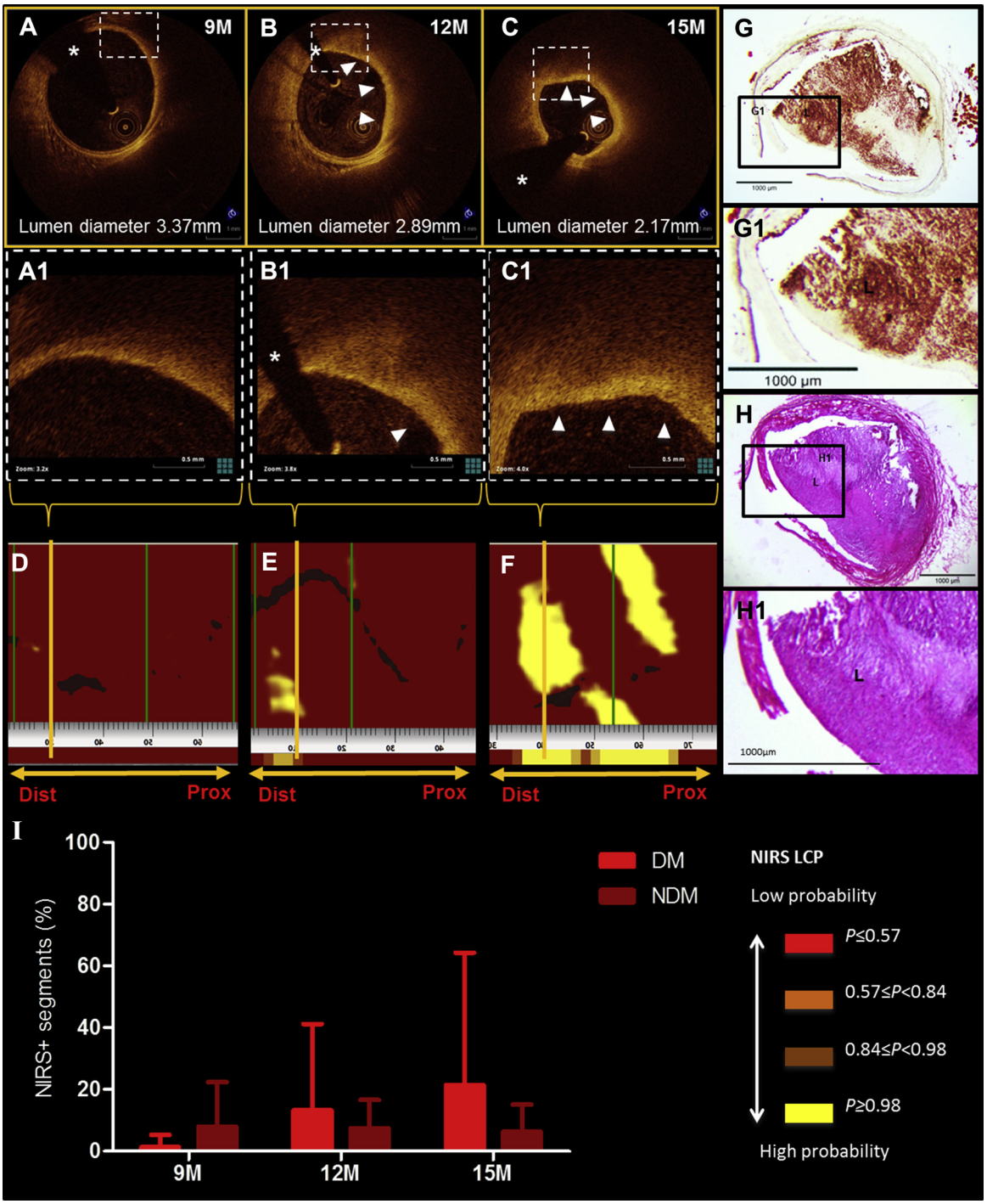

The development of an eccentric LL lesion was observed by OCT **(A to C, arrowheads)** and NIRS **(D to F, yellow)** from 9 (9M) to 12 (12M) and 15 (15M) months. The OCT cross-sections **(A to C)** correspond to the region in the NIRS chemograms **(D to F)**, shown by the **orange lines**. At 15 months, a high lipid burden was detected by OCT **(C, arrowheads)** and NIRS **(F, yellow)**. Histological analysis **(G and H)** of sequential sections stained with Oil red-O **(G)** and hematoxylin and eosin **(H)** stain confirmed the development of an eccentric atheromatous plaque with a large lipid pool **(L in G1 and H1)**. The percentage of NIRS-positive segments increased over time in both FF-DM and FF-NDM swine **(I)**. The graph shows the mean percentage of NIRS-positive segments per swine. Dist = distal; Prox = proximal; LCP = lipid core plaque; LL = lipid laden; other abbreviations as in Figure 1.

FIGURE 5 Concentration Response Curves to BK, SNAP, and ET-1

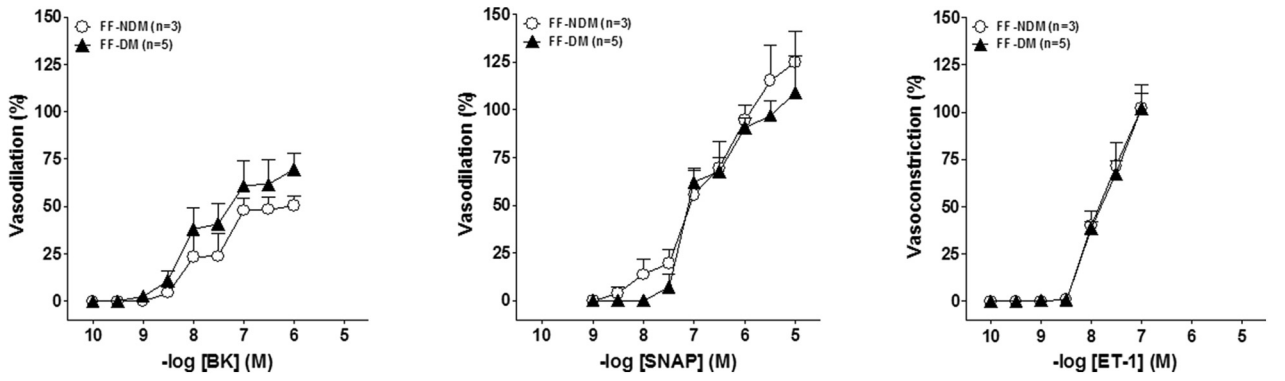

Concentration response curves to BK **(left)**, SNAP **(middle)**, and ET-1 **(right)** of coronary segments of FF-DM and FF-NDM swine. No significant differences in vasodilatory or vasoconstrictor responses were noted. BK = bradykinin; ET = endothelin; SNAP = *S*-nitroso-*N*-acetylpenicillamine; other abbreviations as in Figure 1.

calcified burden that increased from 2 lesion-positive quadrants at 9 months to 3 lesion-positive quadrants at 15 months. Of the 115 segments analyzed at 9 months (n = 74 FF-DM; n = 41 FF-NDM), 17% demonstrated FIT and 8% LL. From 9 to 15 months, the prevalence of disease increased in FF-DM and FF-NDM (Figures 2B to 2D). At 12 months, 28% of subsegments displayed FIT and 18% LL. At 15 months, 40% demonstrated FIT and 21% LL. Similarly, lesion burden increased, indicated by the increased number of lesion-positive quadrants (Figures 2B to 2D). Hence, lipid burden increased, but no OCT-derived thin-cap fibroatheroma developed in any swine (mean cap thickness: 0.21 ± 0.00 mm in FF-DM; 0.18 ± 0.00 mm in FF-NDM; $p > 0.10$; minimal cap thickness: 0.07 mm in FF-DM; 0.10 mm in FF-NDM at 15 months).

Similar to the OCT results that demonstrated an increase in LL appearance (7% to 21%) and lipid burden, NIRS demonstrated an increase in the probability that LCP was present from 9 to 15 months (3% to 12% NIRS-positive subsegments) (Figure 4). Agreement between OCT and NIRS for the presence of lipid-containing lesions was moderate ($\kappa = 0.56$).

CCTA documented a single low-density lesion (186.0 ± 38.3 HU) in the swine that died during the intracoronary imaging procedure at 15 months (Supplemental Figure 2). In the remaining swine, CCTA was unable to detect any coronary lesion, despite the fact that OCT and NIRS showed the development of calcified lesions or lipid-containing lesions, respectively.

EX VIVO FINDINGS. Vascular function. The contractile response to the endothelium-independent vasoconstrictor (U46619) was not different between FF-DM and FF-NDM at 12 months (91 ± 47 mm vs. 98 ± 45 mm, respectively; $p > 0.10$). Coronary segments dilated to endothelium-dependent and -independent vasodilators (BK and SNAP) in a concentration-dependent manner. FF-DM swine demonstrated a reduced response to the endothelium-dependent vasodilator BK similar to that of FF-NDM swine (pEC50: FF-DM 7.6 ± 0.5 vs. FF-NDM 7.7 ± 0.3; $p > 0.10$). The response to the endothelium-independent vasodilator SNAP remained unaltered in FF-DM and FF-NDM ($p > 0.10$), and the response to the endothelium-dependent vasoconstrictor ET-1 was increased (Emax FF-DM: 102 ± 18 vs. FF-NDM: 102 ± 22; $p > 0.10$) (Figure 5).

Histology. Of the swine that died during the imaging procedure, histological analysis demonstrated an eccentric atherosclerotic lesion with necrotic core in the distal left circumflex coronary artery (Supplemental Figure 3). In the remaining swine, coronary atherosclerosis was heterogeneously divided between and within swine, ranging from early (Figure 2A4) to more advanced atherosclerosis (Figures 2A5 and 2A6), as was also documented by OCT (Figure 2).

Substantial aortic atherosclerosis developed in all swine at 12 months (72 ± 6% surface area covered by plaque in FF-DM and 58 ± 12% in FF-NDM) and at 15 months (67 ± 9% FF-DM and 46 ± 31% FF-NDM; $p > 0.10$) (Supplemental Figure 4). There was no correlation between the percentage of aortic

atherosclerosis and triglyceride (R^2: 0.12; p = 0.24), TC (R^2 0.26; p = 0.08), LDL (R^2 0.22; p = 0.11) or HDL levels (R^2: 0.25; p = 0.09). Furthermore, there was no relationship between abdominal aortic atherosclerosis and coronary atherosclerosis. The R^2 value was 0.01 (p = 0.73) for aortic atherosclerosis compared with that for any lesion observed by OCT, and R^2 was 0.10 (p = 0.34) for aortic atherosclerosis compared to that for NIRS-positive lesions.

DISCUSSION

We present a longitudinal, multimodal imaging study assessing early atherosclerosis development in FF-DM and FF-NDM swine. OCT, NIRS, vascular function, and histology demonstrated no differences in early atherosclerosis development between FF-DM and FF-NDM swine. OCT and NIRS enabled the detailed assessment of early coronary atherosclerosis, demonstrating focal lesions that were highly variable in presence, location, and morphology in all swine, whereas CCTA was not able to detect these discrete early atherosclerotic changes.

ATHEROSCLEROSIS DEVELOPMENT IN FF-DM VERSUS FF-NDM SWINE. As expected, coronary and aortic atherosclerosis progressed in all swine over time. In line with findings by Fernandez-Friera et al. (14), who demonstrated variable distribution of subclinical atherosclerosis in coronary arteries and aortae of middle-aged patients, we observed no correlation between aortic and coronary atherosclerosis within swine. Furthermore, a gene expression study demonstrated that inflammatory genes were markedly upregulated in coronary arteries compared with aorta from the same animal, potentially explaining the different atherosclerosis development in the different vascular beds (15).

Between FF-DM and FF-NDM swine, there were no significant differences in extent or morphology of atherosclerosis as assessed by intracoronary imaging, and there were no differences in endothelium-dependent and independent vasodilation. This might indicate a final common pathway in the atherosclerotic disease process, as has also recently been described in a mini-pig model, with a similar atherosclerosis development in DM and NDM swine (16). However, Duff et al. (17) was one of the first to assess experimental atherosclerosis and suggested that hyperglycemia served as a protective factor against the development of experimental atherosclerosis in rabbits. The differences between our study findings and those by Duff et al. (17) regarding the effect of hyperglycemia on the development of atherosclerosis may be explained by several factors, including species differences, duration of DM, the toxins used to induce DM, and the type and amount of diet given to the swine (18).

First, rabbits are highly responsive to cholesterol manipulation and develop lesions in a fairly short time. Lesions are generally fattier and more macrophage rich than human lesions (19). Swine, on the other hand, develop spontaneous coronary atherosclerosis similar to humans (4). Second, follow-up by Duff et al. (17) reached up to 4 months, whereas we followed the FF-DM and FF-NDM swine from 9 months to either 12 or 15 months. The protective effect of hyperglycemia might only have been apparent in the early stages of the disease. This observation of protection against atherosclerosis development is in line with observations by Niccoli et al. (20), who demonstrated that diabetic patients experience their first event at a later stage of atherosclerotic disease than nondiabetic patients. Third, Duff et al. (17) used alloxan to render the rabbits diabetic, whereas we used a single-dose injection of streptozotocin. Differences in the toxin used to induce DM might have resulted in noncomparable atherosclerosis development. Fourth, we fed our swine twice daily but monitored individual caloric intake to maintain similar growth patterns, whereas Duff et al. (17) fed their rabbits ad libitum. Monitoring individual caloric intake might have accounted for similar atherosclerosis development in FF-DM and FF-NDM swine.

Interestingly, DM was associated with accelerated atherogenesis under comparable conditions of hyperlipidemia in other swine models. Moreover, Dixon et al. (21) and Gerrity et al. (22) demonstrated enhanced lesion development in diabetic hyperlipidemic swine. The differences between our findings of a similar atherosclerosis development between FF-DM and FF-NDM swine and the findings by Dixon et al. (21) and Gerrity et al. (22) may also be explained by differences in species, duration of diabetic disease, toxins used to induce diabetes mellitus, and type and amount of diet given to the swine (18). Dixon et al. (21) used male Sinclair miniature swine and induced diabetes mellitus by using alloxan, whereas Gerrity et al. (22) used Yorkshire swine and induced diabetes by using 50 mg/kg streptozotocin each day for 3 days; we used crossbred Yorkshire × Landrace swine and induced diabetes by a single-dose injection of 140 mg/kg streptozotocin.

Furthermore, Gerrity et al. (22) fed the swine ad libitum in the beginning of the study, whereas we fed our swine twice daily and monitored individual caloric intake to achieve similar growth patterns. This might have resulted in similar atherosclerosis development in the FF-DM and FF-NDM swine in our study.

Because our swine demonstrated lipid profiles similar to those of the swine studied by Gerrity et al. (22) and Dixon et al. (21) but demonstrated different patterns of atherosclerosis development, we believe that hypercholesterolemia, with or without hyperglycemia, is not the only factor contributing to the development of atherosclerosis in these animal models.

Factors such as duration of DM and hypertension may attribute to the severity of atherosclerotic disease. Moreover, hypertension, not present in the current study, has been associated with adverse atherosclerosis-related events in DM patients (23). Future studies in atherosclerotic swine should consider using older-aged swine and include risk factors such as hypertension to accurately evaluate development of advanced coronary atherosclerosis.

COMPARISON OF IMAGING TECHNIQUES. Over time, the prevalence and extent of disease increased in FF-DM and FF-NDM swine as detected by OCT and NIRS. OCT demonstrated increasing LL appearance and lipid burden (**Figure 2**), and NIRS demonstrated an increase in the probability that LCP was present from 9 to 15 months (**Figure 4**). Interestingly, a moderate agreement was observed between OCT and NIRS for the detection of lipid. This finding is in line with a previously published study that demonstrated a moderate correlation between OCT and NIRS for detection of lipid and measurement of lipid contents (24). In contrast to OCT, which visualizes vessel structure and thus lipid morphology directly, NIRS provides calculated values of the probability of lipid in each pixel on the vessel surface (9). This difference in data acquisition may contribute to the moderate correlation between the 2 modalities.

CCTA did not detect any of the lesions documented by OCT or NIRS. Subtle differences in tissue contrast were not noted because most of the lesions were small, nonobstructive, and noncalcified, with a lesion burden of 1 to 2 lesion-positive quadrants. Moreover, the small nonobstructive coronary plaques observed in our swine appeared to be beyond the resolution of the technology (25). In previous studies, CT emerged as a noninvasive technique to exclude coronary artery disease and demonstrated good accuracy for detection of coronary artery stenosis and assessment of high-density and low-density lesions (10,26). However, CCTA is limited by the fact that the image contrast between plaque and other soft tissues (e.g., FIT) is small (27). This may affect identification and sizing of coronary plaque and most likely explains the inability of CCTA to detect the mainly noncalcified lesions in the present study.

OCT, NIRS, and CCTA acquire data differently and thus provide different types of information, which can be complementary and highly valuable for evaluating atherosclerosis development (28).

STUDY LIMITATIONS. Sample size was relatively small, especially at 15 months. To study differences in vascular function and histology over several time points, sacrifice of a small number of swine was mandatory. Furthermore, differences remain between swine and human. Although swine, like humans, develop spontaneous coronary atherosclerosis, in the present study, swine were relatively young and thus did not develop advanced atherosclerosis, as can be observed in older-aged patients who suffer from hypercholesterolemia and/or DM for a longer time period. However, the aim of our study was to assess the effect of DM on early atherosclerosis development.

CONCLUSIONS

Our swine model allowed assessment of early coronary atherosclerosis development using intracoronary OCT and NIRS. CCTA could not detect early atherosclerotic lesions, but OCT and NIRS demonstrated a similar gradual development of early atherosclerosis in FF-DM and FF-NDM swine. Moreover, OCT, NIRS, vascular function, and histology demonstrated no differences in early atherosclerosis development between FF-DM and FF-NDM swine up to 15 months.

ACKNOWLEDGMENTS Dedicated to Prof. Dr. W.J. van der Giessen, who helped to design and conduct this preclinical study, but passed away before its completion.

REPRINT REQUESTS AND CORRESPONDENCE: Dr. Evelyn Regar, Department of Cardiology, Thoraxcenter, BA-585, Erasmus University Medical Centre, "s-Gravendijkwal 230, 3015 CE Rotterdam, the Netherlands. E-mail: e.regar@erasmsumc.nl.

PERSPECTIVES

COMPETENCY IN MEDICAL KNOWLEDGE: The number of patients with DM increases every year, and these individuals have a 2- to 6-fold increased risk of encountering atherosclerosis-related events compared with non-DM patients. Early detection of anatomic and functional atherosclerotic changes seems warranted. However, patients typically present to the clinician with advanced atherosclerotic disease, thus complicating the study of early atherosclerosis development. The swine coronary artery model may offer advantages: 1) the anatomy and physiology of swine heart are similar to those of human hearts; 2) swine can be rendered diabetic by injection of streptozotocin; 3) patient-like spontaneous coronary atherosclerosis development can be mimicked by additionally feeding the swine a high-cholesterol, high-sugar diet; 4) in vivo longitudinal invasive and noninvasive imaging can be performed; 5) ex vivo coronary endothelial function can be tested; and 6) histology can be performed to assess the magnitude of coronary atherosclerosis at different time points. Moreover, the swine coronary artery model can help improve our understanding of the effect of DM on the development of coronary atherosclerosis, which may modulate medical therapeutic strategies and thereby enhance prevention of cardiovascular events in the clinical setting.

TRANSLATIONAL OUTLOOK: To enable development of new therapeutic strategies and to reduce the health care burden, we believe that it is important to increase our understanding of early coronary atherosclerosis development. However, because patients suffering coronary artery disease typically present to the clinician relatively late, with advanced stages of disease, we used a swine coronary artery model suitable for evaluation of human-like coronary artery disease development. Interestingly, our study showed that hypercholesterolemia or hyperglycemia were not the only predictors of coronary atherosclerosis development in swine. Future studies in atherosclerotic swine should consider using older-aged swine and include additional risk factors such as hypertension. Furthermore, we were able to demonstrate that a number of coronary imaging techniques, including OCT, NIRS, and CCTA, can be consecutively used for longitudinal assessment of the atherosclerotic disease process, which may offer the possibility for future studies in a reduced number of animals.

REFERENCES

1. Norhammar A, Malmberg K, Diderholm E, et al. Diabetes mellitus: the major risk factor in unstable coronary artery disease even after consideration of the extent of coronary artery disease and benefits of revascularization. J Am Coll Cardiol 2004;43:585–91.

2. Wu KK, Huan Y. Diabetic atherosclerosis mouse models. Atherosclerosis 2007;191:241–9.

3. Skold BH, Getty R, Ramsey FK. Spontaneous atherosclerosis in the arterial system of aging swine. Am J Vet Res 1966;27:257–73.

4. van Ditzhuijzen NS, van den Heuvel M, Sorop O, et al. Invasive coronary imaging in animal models of atherosclerosis. Neth Heart J 2011;19:442–6.

5. van den Heuvel M, Sorop O, Koopmans SJ, et al. Coronary microvascular dysfunction in a porcine model of early atherosclerosis and diabetes. Am J Physiol Heart Circ Physiol 2012;302:H85–94.

6. Guide for the Care and Use of Laboratory Animals. 8th edition. Washington, DC: National Academies Press, 2011.

7. Tearney GJ, Regar E, Akasaka T, et al. Consensus standards for acquisition, measurement, and reporting of intravascular optical coherence tomography studies: a report from the International Working Group for Intravascular Optical Coherence Tomography Standardization and Validation. J Am Coll Cardiol 2012;59:1058–72.

8. Prati F, Regar E, Mintz GS, et al. Expert review document on methodology, terminology, and clinical applications of optical coherence tomography: physical principles, methodology of image acquisition, and clinical application for assessment of coronary arteries and atherosclerosis. Eur Heart J 2010;31:401–15.

9. Gardner CM, Tan H, Hull EL, et al. Detection of lipid core coronary plaques in autopsy specimens with a novel catheter-based near-infrared spectroscopy system. J Am Coll Cardiol Img 2008;1:638–48.

10. Motoyama S, Kondo T, Sarai M, et al. Multislice computed tomographic characteristics of coronary lesions in acute coronary syndromes. J Am Coll Cardiol 2007;50:319–26.

11. van den Heuvel M, Sorop O, Batenburg WW, et al. Specific coronary drug-eluting stents interfere with distal microvascular function after single stent implantation in pigs. J Am Coll Cardiol Intv 2010;3:723–30.

12. Batenburg WW, de Vries R, Saxena PR, Danser AH. L-S-nitrosothiols: endothelium-derived hyperpolarizing factors in porcine coronary arteries? J Hypertens 2004;22:1927–36.

13. Batenburg WW, Popp R, Fleming I, et al. Bradykinin-induced relaxation of coronary microarteries: *S*-nitrosothiols as EDHF? Br J Pharmacol 2004;142:125–35.

14. Fernandez-Friera L, Penalvo JL, Fernandez-Ortiz A, et al. Prevalence, vascular distribution, and multiterritorial extent of subclinical atherosclerosis in a middle-aged cohort: the PESA (Progression of Early Subclinical Atherosclerosis) study. Circulation 2015;131:2104–13.

15. Mohler ER III, Sarov-Blat L, Shi Y, et al. Site-specific atherogenic gene expression correlates with subsequent variable lesion development in coronary and peripheral vasculature. Arterioscler Thromb Vasc Biol 2008;28:850–5.

16. Ludvigsen TP, Kirk RK, Christoffersen BO, et al. Gottingen minipig model of diet-induced atherosclerosis: influence of mild streptozotocin-induced diabetes on lesion severity and markers of inflammation evaluated in obese, obese and diabetic, and lean control animals. J Transl Med 2015;13:312.

17. Duff GL, Mc MG. The effect of alloxan diabetes on experimental cholesterol atherosclerosis in the rabbit. J Exp Med 1949;89:611–30.

18. Granada JF, Kaluza GL, Wilensky RL, Biedermann BC, Schwartz RS, Falk E. Porcine models of coronary atherosclerosis and vulnerable

plaque for imaging and interventional research. EuroIntervention 2009;5:140–8.

19. Badimon L. Atherosclerosis and thrombosis: lessons from animal models. Thromb Haemost 2001;86:356–65.

20. Niccoli G, Giubilato S, Di Vito L, et al. Severity of coronary atherosclerosis in patients with a first acute coronary event: a diabetes paradox. Eur Heart J 2013;34:729–41.

21. Dixon JL, Stoops JD, Parker JL, Laughlin MH, Weisman GA, Sturek M. Dyslipidemia and vascular dysfunction in diabetic pigs fed an atherogenic diet. Arterioscler Thromb Vasc Biol 1999;19:2981–92.

22. Gerrity RG, Natarajan R, Nadler JL, Kimsey T. Diabetes-induced accelerated atherosclerosis in swine. Diabetes 2001;50:1654–65.

23. Raggi P, Shaw LJ, Berman DS, Callister TQ. Prognostic value of coronary artery calcium screening in subjects with and without diabetes. J Am Coll Cardiol 2004;43:1663–9.

24. Yonetsu T, Suh W, Abtahian F, et al. Comparison of near-infrared spectroscopy and optical coherence tomography for detection of lipid. Catheter Cardiovasc Interv 2014;84:710–7.

25. van der Giessen AG, Toepker MH, Donelly PM, et al. Reproducibility, accuracy, and predictors of accuracy for the detection of coronary atherosclerotic plaque composition by computed tomography: an ex vivo comparison to intravascular ultrasound. Invest Radiol 2010;45:693–701.

26. Miller JM, Rochitte CE, Dewey M, et al. Diagnostic performance of coronary angiography by 64-row CT. N Engl J Med 2008;359:2324–36.

27. Halliburton SS, Schoenhagen P, Nair A, et al. Contrast enhancement of coronary atherosclerotic plaque: a high-resolution, multidetector-row computed tomography study of pressure-perfused, human ex-vivo coronary arteries. Coronary artery disease 2006;17:553–60.

28. Koskinas KC, Ughi GJ, Windecker S, Tearney GJ, Raber L. Intracoronary imaging of coronary atherosclerosis: validation for diagnosis, prognosis and treatment. Eur Heart J 2016;37:524–35.

KEY WORDS animal model, coronary artery disease, coronary computed tomography angiography, diabetes mellitus, near-infrared spectroscopy, optical coherence tomography

APPENDIX For an expanded methods section as well as supplemental figures and table, please see the online version of this article.